Arteriosclerosis, Thrombosis, and Vascular Biology

ORIGINAL RESEARCH

Capacity for LDL (Low-Density Lipoprotein) Retention Predicts the Course of Atherogenesis in the Murine Aortic Arch

Esmeralda A. Lewis, Rocío Muñiz-Anquela, Ibon Redondo-Angulo, Leticia González-Cintado, Verónica Labrador-Cantarero, Jacob F. Bentzon

BACKGROUND: To cause atherosclerosis, LDLs (low-density lipoproteins) must first pass through the endothelium and then become retained in the arterial matrix. Which of these two processes is rate-limiting and predicts the topography of plaque formation remains controversial. To investigate this issue, we performed high-resolution mapping of LDL entry and retention in murine aortic arches before and during atherosclerosis development.

METHODS: Maps of LDL entry and retention were created by injecting fluorescently labeled LDL followed by near-infrared scanning and whole-mount confocal microscopy after 1 hour (entry) and 18 hours (retention). By comparing arches between normal mice and mice with short-term hypercholesterolemia, we analyzed changes in LDL entry and retention during the LDL accumulation phase that precedes plaque formation. Experiments were designed to secure equal plasma clearance of labeled LDL in both conditions.

RESULTS: We found that LDL retention is the overall limiting factor for LDL accumulation but that the capacity for LDL retention varied substantially over surprisingly short distances. The inner curvature region, previously considered a homogenous atherosclerosis-prone region, consisted of dorsal and ventral zones with high capacity and a central zone with low capacity for continued LDL retention. These features predicted the temporal pattern of atherosclerosis, which first appeared in the border zones and later in the central zone. The limit to LDL retention in the central zone was intrinsic to the arterial wall, possibly caused by saturation of the binding mechanism, and was lost upon conversion to atherosclerotic lesions.

CONCLUSIONS: Capacity for continued LDL retention varies over short distances and predicts where and when atherosclerosis develops in the mouse aortic arch.

GRAPHIC ABSTRACT: A graphic abstract is available for this article.

Key Words: animals ■ atherosclerosis ■ endothelium ■ hypercholesterolemia ■ mice

LDLs (low-density lipoproteins) and other APOB (apolipoprotein B)-containing lipoproteins cause atherosclerotic lesions and their ischemic complications.[1] Although LDLs are ubiquitous in the body, LDL accumulation and atherogenesis localize initially near arterial bends and branching points, with other regions affected only later or not at all. Uncertainty remains about the mechanism underlying these topographical differences.[2]

For LDLs to accumulate in the arterial intima, they must cross the endothelium by transcytosis or through intercellular slits (LDL entry) and be retained by binding to proteoglycans or precipitation by local enzymes (LDL retention).[2–4] Both processes have been proposed as the rate-limiting step in early atherogenesis, but there is little experimental evidence to support either view.

See accompanying editorial on page 650

Previous studies used radioactive labeling to map LDL entry and retention, but the results were inconsistent.[5,6] Radioactive techniques are quantitative but have low resolution. Since atherosclerosis initiation is at first a

Correspondence to: Jacob F. Bentzon, MD, PhD, Centro Nacional de Investigaciones Cardiovasculares Carlos III, Calle Melchor Fernández Almagro, 3 28029 Madrid, Spain. Email jfbentzon@cnic.es

Supplemental Material is available at https://www.ahajournals.org/doi/suppl/10.1161/ATVBAHA.122.318573.
For Sources of Funding and Disclosures, see page 649.

Arterioscler Thromb Vasc Biol is available at www.ahajournals.org/journal/atvb

Nonstandard Abbreviations and Acronyms

APOB	apolipoprotein B
ASO	antisense oligonucleotide
HC	high cholesterol
LDL	low-density lipoprotein
PCSK9	proprotein convertase subtilisin/kexin type 9
rAAV	recombinant adeno-associated virus

microscopic phenomenon, we hypothesized that increasing the spatial resolution of LDL-tracking techniques would provide new insights into the processes that drive LDL accumulation at some but not other sites.

Here, we mapped the entry and retention of fluorescently labeled LDL at a high-resolution before and during atherogenesis in the aortic arch. We found that LDL retention is rate-limiting for LDL accumulation, but LDL-retaining regions are further subdivided by their capacity for continued LDL accumulation under hypercholesterolemic conditions. These differences predicted the course of lesion development within the atherosclerosis-prone inner curvature region.

Highlights

- High-resolution maps of LDL (low-density lipoprotein) entry and retention across the murine aortic arch reveal functional differences over surprisingly short distances within the atherosclerosis-prone inner curvature region.
- LDL retention is the rate-limiting process for LDL accumulation in all subregions, but the retention capacity varies.
- High capacity for continued LDL retention characterizes the ventral and dorsal border zones of the inner curvature region, which are also the first to recruit macrophages and develop atherosclerosis. The central zone of the inner curvature region shows transient saturation of LDL retention and develops atherosclerosis only later.

METHODS

Data are available from the corresponding author upon request. RNA sequencing data have been deposited in Gene Expression Omnibus (accession number GSE210096). The main procedures are described below. An expanded methods section can be found in the Supplemental Material

Animal Experiments

Animal experiments were reviewed by institutional committees and approved by the Comunidad de Madrid (PROEX 266/16). Mice were wild-type C57BL/6J males originating from The Jackson Laboratory (Bar Harbor, Maine). One sex was used to optimize statistical power, and males were chosen because of slower atherogenesis,[7] which provides more time to study the steps in disease initiation. Unless noted otherwise, animals were 8 weeks of age at the start of experiments.

LDL levels were increased using a tail vein injection of recombinant adeno-associated virus (serotype 8) encoding gain-of-function (D377Y) mouse PCSK9 (proprotein convertase subtilisin/kexin type 9; recombinant adeno-associated virus [rAAV]; 10^{11} vector genomes) followed by feeding on a high cholesterol (HC) diet (0.3% cholesterol, 4.2% fat, S9167-E0150, Sniff, Soest, Germany) as previously described.[8] LDL levels were decreased to approximately normal levels using intraperitoneal injections of locked nucleic acid antisense oligonucleotides targeting apolipoprotein B mRNA (*ApoB* antisense oligonucleotide [ASO], Qiagen, Hilden, Germany) as previously described.[9] Mismatched control oligonucleotides (*Ctrl* ASO, Qiagen) were used in control mice. Unless noted otherwise, the dose of each was 5 mg/kg. By nearly abolishing hepatic LDL receptor protein expression, this experimental system equalizes the fractional catabolic rate of plasma LDL by the liver between hypercholesterolemic and normocholesterolemic mice. Using these tools to increase and normalize plasma LDL levels, the following 11 experiments were performed (group sizes noted in figure legends):

1. To evaluate arterial accumulation of endogenous LDL during atherogenesis, mice received rAAV-PCSK9 and were fed on the HC diet for 0, 2, 4, 6, or 12 weeks (*study 1*). Ascending aortas and aortic roots were sectioned and immunostained for the protein moiety of LDL, APOB.
2. To compare entry and retention of exogenous labeled LDL in normocholesterolemic and hypercholesterolemic mice in the setting of equal hepatic LDL clearance, mice received rAAV-PCSK9 and were fed on HC diet for 3.5 weeks. Half of the mice were injected with *ApoB* ASO at 0, 1, 2, and 3 weeks to maintain normal LDL levels. The others received *Ctrl* ASO. This experiment was repeated multiple times, and the aortic arches were analyzed for entry and retention of exogenous labeled LDL (*studies 2* and *4*), expression of known LDL-interacting proteins (*study 7*), gene expression by RNA-seq analysis (*study 8*), accumulation of endogenous LDL by staining for APOB (*study 9*), and distribution of macrophages (post-staining of arches from *study 4*).
3. To measure LDL entry and retention during the first weeks of hypercholesterolemia, mice received rAAV-PCSK9 and began HC diet at 8, 10, or 11 weeks of age (*study 3*). After 4, 2, or 1 week of hypercholesterolemia, rates of entry and retention of exogenous labeled LDL were measured (at 12 weeks of age).
4. To increase or remove competition from endogenous circulating LDLs before measuring the retention of exogenous labeled LDL, we briefly induced (*study 5*) or corrected hypercholesterolemia (*study 6*). In the brief hypercholesterolemia experiment, mice received rAAV-PCSK9 and a dose of either *ApoB* ASO or *Ctrl* ASO followed by 3 days of HC diet. In the hypercholesterolemia correction experiment, rAAV-PCSK9-treated mice were fed on HC diet and injected with *ApoB* ASO at 0, 1, 2, and 3 weeks or with *Ctrl* ASO at 0, 1, and 2 weeks followed by a final high (10 mg/kg) dose of *ApoB* ASO at 3 weeks.

5. To analyze the topography of lesion development in the aortic arch, mice received rAAV-PCSK9 and were fed on HC diet for 0, 4, 6, 12, or 24 weeks (*study 10*). Aortas were opened and examined by stereomicroscopy.
6. To assess whether there is competition among LDLs for retention in atherosclerotic plaques, rAAV-PCSK9-injected mice were fed on HC diet for 12 weeks (*study 11*). One week before the end point, mice received a high (10 mg/kg) dose of either *ApoB* ASO (to lower LDL levels) or *Ctrl* ASO (to maintain high LDL levels). Exogenous labeled LDLs were injected 18 hours before the endpoint, and the ascending aortas were sectioned and analyzed by confocal microscopy.

Preparation and Administration of Exogenous Labeled LDL

Blood was drawn from healthy human volunteers, and LDL was purified and labeled with Atto680-, Atto647-, or Atto565-N-hydroxysuccinimide esters that attach to the free amines on APOB. The names of the Atto labels indicate their peak excitation (absorption) wavelengths in nm. The ethical committee of Instituto de Salud Carlos III approved the study (CEI PI 12_2016-v2).

Exogenous labeled LDLs were injected into mice through the tail vein, and animals were euthanized and perfusion-fixed after 1 hour (to measure LDL entry) or after 18 hours (to measure LDL retention). To measure both arterial entry and retention of exogenous LDLs in the same mouse, we used LDLs labeled with two different fluorophores injected 17 hours apart.

Maps of LDL Entry and Retention

High-resolution maps of exogenous labeled LDL in the aortic intima were created by 2 techniques. For high-throughput analysis, we conducted near-infrared scanning of the aortic luminal surface after injection with Atto680-LDL. Thoracic aortas were opened longitudinally (along the outer and inner curvatures of the arch and down the front of the descending aorta), mounted on slides, and scanned (luminal surface down) on a LiCor Odyssey Infrared Imaging System. We have previously published the details of this technique,[10] but in preparation for the present study, we conducted two additional validation experiments. First, we confirmed that the signal was proportional to the amount of exogenous labeled LDL in the artery (Figure S1). Second, we verified that PCSK9 does not directly alter entry or retention of the exogenous labeled LDL, which would complicate the interpretation of the experiments (Figure S2). It should be noted that because entry and retention are measured over different periods of time, the absolute values are not directly comparable.

For increased resolution and simultaneous analysis of exogenous labeled LDL entry and retention, we performed whole-mount confocal microscopy. The aortic arch up to the branch site of the brachiocephalic trunk was extracted and opened along the upper ventral wall to maintain the inner curvature region intact. Whole-mount microscopy of Atto565-LDL and Atto647-LDL in the aortic intima was performed using a Zeiss LSM 780 or Leica SP8 Lightning-Navigator confocal microscope. All quantitative image analysis was performed in Fiji (also known as ImageJ) version 2.0.0-rc-69/1.53c with associated plugins using the workflows outlined in Figures S3 through S7.[11,12]

RESULTS

LDL Accumulation Precedes and Predicts Plaque Development

Previous studies have shown that rabbit arteries quickly accumulate LDLs after the onset of hypercholesterolemia.[13,14] To study the sequence of hypercholesterolemia, intimal LDL accumulation, and plaque formation in mice, we induced hypercholesterolemia by injection of rAAV-PCSK9 followed immediately by the HC diet for 0, 2, 4, 6, or 12 weeks (*study 1*, Figure 1A and 1B). LDL accumulation was quantified in serial sections of the ascending aortic arch by APOB staining (Figure 1C and 1D). After 2 weeks, significant intimal APOB accumulation was detected in a region around the inner curvature (henceforth the *inner curvature region*). This preceded increases in the intimal area, which were not statistically significant before 6 weeks (Figure 1E and 1F). Over the following weeks, lesions developed across the inner curvature region. The aortic wall outside the inner curvature region (henceforth the *outer zone*) did not accumulate LDL or develop lesions. LDL accumulation thus preceded and marked the region that eventually developed plaques. Similar results were obtained in the aortic root (Figure S8).

In the following analyses, we use the term early atherosclerosis for the LDL-accumulating phase that precedes growth of intimal lesions.

Retention Is Rate-Limiting for LDL Accumulation in Early Atherosclerosis

To understand whether entry or retention is rate-limiting for LDL accumulation in early atherosclerosis, we set out to compare the entry and retention rates of Atto680-LDL in short-term hypercholesterolemic and normocholesterolemic mice. We reasoned that the rate-limiting process would be saturated in hypercholesterolemic mice, which would reduce both entry and retention (if entry was rate-limiting) or only retention (if retention was rate-limiting) of Atto680-LDL.

To make an unbiased assessment, we could not simply contrast rAAV-PCSK9-injected and non-injected mice because they would differ in hepatic LDL receptor levels and hence in Atto680-LDL clearance. Therefore, we treated mice with rAAV-PCSK9 and HC diet but kept plasma LDL low in half of them with weekly injections of *ApoB* ASO (*study 2*, Figure 2A and 2B). *ApoB* ASO degrade hepatic *Apob* mRNA and thereby block very-low-density lipoprotein output, leading to lower plasma LDL levels. The other group was treated with *Ctrl* ASO to control for unspecific effects of ASO injections. After 3.5 weeks, mice were injected with Atto680-LDL and then euthanized and perfusion-fixed 1 or 18 hours later. Near-infrared scanning of the opened aorta was

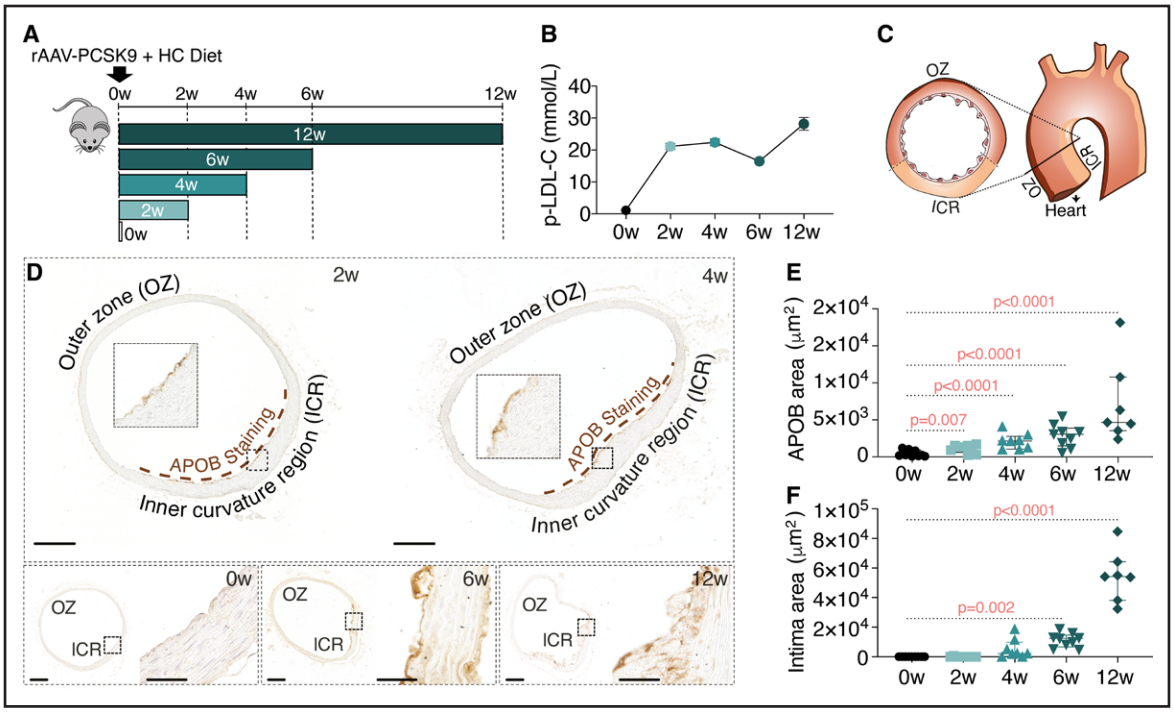

Figure 1. LDL (low-density lipoprotein) accumulation precedes plaque development.
A, Experimental design. Mice were injected with rAAV (recombinant adeno-associated virus)-PCSK9 (proprotein convertase subtilisin/kexin type 9) and fed on high cholesterol (HC) diet for 0, 2, 4, 6, or 12 weeks (n=7 per time point). **B**, Plasma LDL cholesterol concentrations. **C**, Sectioning of the ascending aorta (3 sections analyzed separated by 200 µm). **D**, LDL accumulation detected by APOB (apolipoprotein B) staining (brown). Insets show selected areas at higher magnification. **E** and **F**, Quantification of APOB-stained and intimal areas. All, Graphs show mean±SEM (**B**) or median±interquartile range (**E**, **F**). Data analyzed by 1-way ANOVA of log-transformed data with Dunnett post-test (**E**) or Kruskal-Wallis test with Dunn post-test (**F**) comparing each time point with 0 w. No test performed (**B**). Scale bars, 200 µm in overview and 50 µm in magnified areas ICR indicates inner curvature region; and OZ, outer zone.

conducted to measure LDL entry and retention, respectively (Figure 2C through 2E). The 3.5-week time point was chosen to be well into the LDL-accumulating phase but preceding the growth of intimal lesions.

Entry and retention of Atto680-LDL localized mainly to the inner curvature region, including the lower parts of the dorsal and ventral walls. It was also seen in the proximal part of the main aortic branches. Quantification of total signal intensity showed that global Atto680-LDL entry was higher, while global Atto680-LDL retention was lower in hypercholesterolemic compared with normocholesterolemic mice (Figure 2D and 2E). These observations indicated that retention is the rate-limiting step for global LDL accumulation in early atherosclerosis. Notably, the measurements were done under conditions of equal clearance of Atto680-LDL (Figure 2F).

To corroborate this finding with an alternative approach, we analyzed how LDL entry and retention rates change during the first weeks of hypercholesterolemia. Mice were injected with rAAV-PCSK9 at 8, 9, or 11 weeks of age and fed on the HC diet until 12 weeks of age (*study 3*). The analysis of entry and retention was then performed in all mice with the same batch of Atto680-LDL, allowing direct comparison (Figure 2G and 2H). We found that global trans-endothelial entry of Atto680-LDL were increased within just 2 weeks of hypercholesterolemia (Figure 2I), despite the increased levels of endogenous LDL competing for the same process; yet increased entry did not increase the retention of Atto680-LDL (Figure 2J). This result confirms that the rate of LDL retention, but not that of LDL entry, is the limiting factor for global LDL accumulation in early atherosclerosis.

The Capacity for LDL Retention Varies Within the Inner Curvature Region

Inspection of the near-infrared scans in Figure 2E suggested that not only the global level but also the pattern of retention was altered in early atherosclerosis. Normal aortas showed relatively uniform Atto680-LDL retention across the inner curvature region, but aortas from hypercholesterolemic mice had notably less Atto-680-LDL retention in the central part of the inner curvature (where the arch was cut open for scanning) compared with neighboring parts. The central zone with reduced retention was not present in the most proximal part of the ascending aorta and grew toward the level of the brachiocephalic trunk. This appeared to be the case whether looking at the left (dorsal) or right (ventral) section of the opened aortic arch, giving the LDL retention signal in hypercholesterolemic mice a V-shaped appearance.

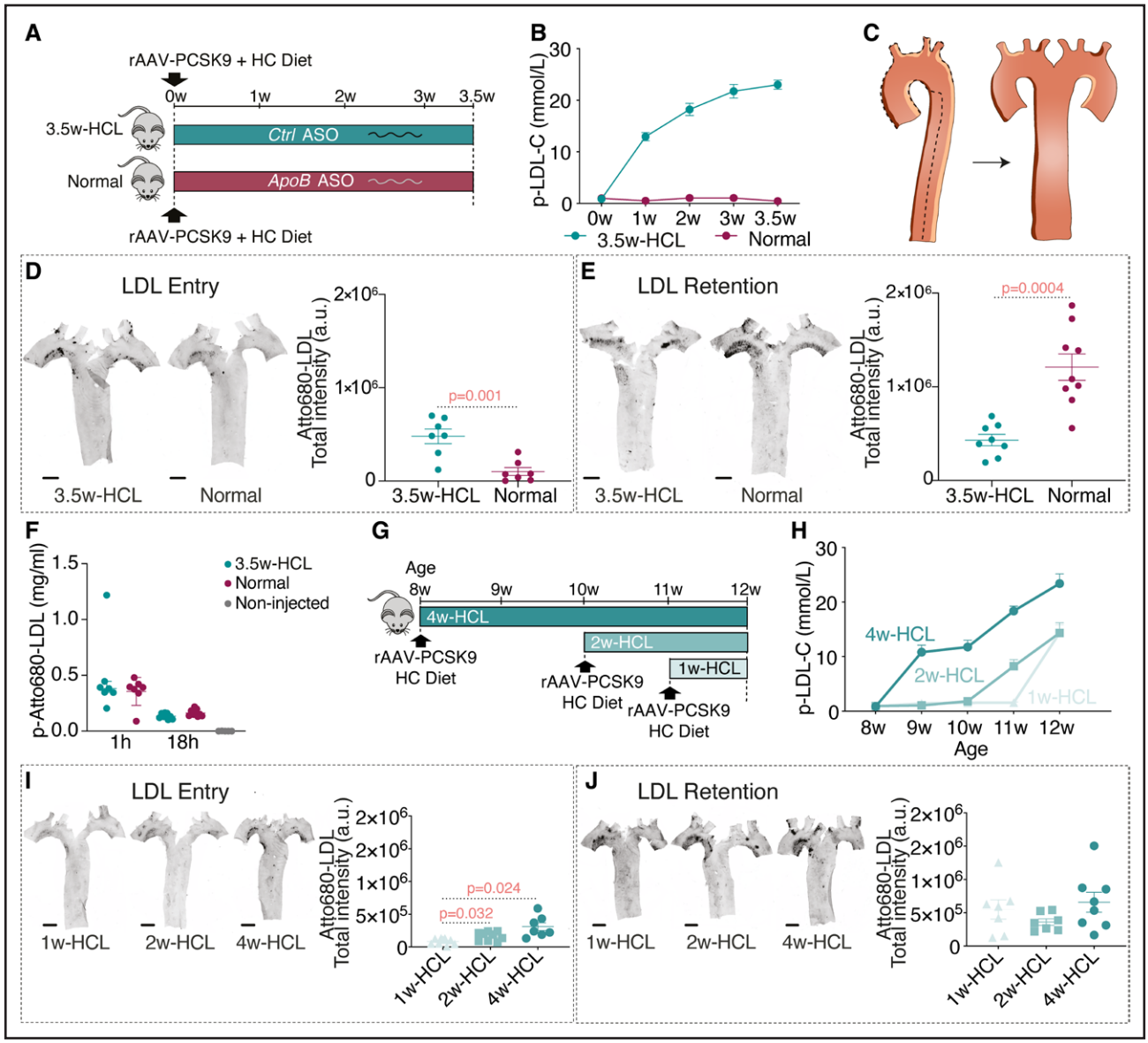

Figure 2. Retention is rate-limiting for LDL (low-density lipoprotein) accumulation.
A, Experimental design. Mice were injected with rAAV (recombinant adeno-associated virus)-PCSK9 (proprotein convertase subtilisin/kexin type 9), started on the high cholesterol (HC) diet, and maintained for 3.5 weeks at high LDL (3.5w-HCL, n=15) or normal LDL (normal, n=16) using weekly injections of *Ctrl* ASO or *ApoB* ASO, respectively. **B**, Plasma LDL cholesterol concentrations. **C**, Opening of the aorta for the near-infrared scans. **D** and **E**, Representative near-infrared scans and quantification of total Atto680-LDL entry and retention in aortas from 3.5w-HCL and normal mice (n=7–9 per group). **F**, Plasma Atto680-LDL levels were similar between 3.5w-HCL and normal groups euthanized at 1 hours and at 18 hours indicating similar hepatic LDL clearance rates. Non-injected mice (n=5) provided negative controls. **G**, Experimental design. Hypercholesterolemia was induced by rAAV-PCSK9 injection and HC diet and maintained for 1, 2, or 4 weeks before analysis of LDL entry and retention (1w-HCL, 2w-HCL, and 4w-HCL, n=7–9 per group). **H**, Plasma LDL cholesterol concentrations. **I** and **J**, Representative near-infrared scans and quantification of total Atto680-LDL entry and retention after 1, 2, and 4 weeks of hypercholesterolemia. All, Graphs show mean±SEM (**D**, **E**, **H**, **I**, **J**) or median±interquartile range (**F**). Data analyzed by *t* test (**D**), Welch *t* test (**E**), Mann-Whitney *U* test (**F**), or Brown-Forsythe ANOVA test with Dunnet T3 post-tests (**I** and **J**). No test performed (**B** and **H**). Scale bars, 1 mm. HCL indicates hypercholesterolemia.

To quantify this, we subdivided the inner curvature region into a *central zone* (near to and including the inner curvature) and *dorsal* and *ventral border zone*s (on the lower part of the dorsal and ventral walls) as indicated schematically in Figure 3A. The remainder was the *outer zone*. We then re-analyzed the near-infrared scans from Figure 2 of the left (dorsal) section of the opened aortic arch that contains part of the central zone, the dorsal border zone, and part of the outer zone. As suspected, Atto680-LDL retention was significantly reduced in the central zone but maintained in the dorsal border zone in early atherosclerotic compared with normal aortas (Figure 3B). This subdivision also revealed clear differences in Atto680-LDL entry. Entry was increased in the dorsal border zone of early atherosclerotic compared with normal aortas but was similar between groups in the central zone.

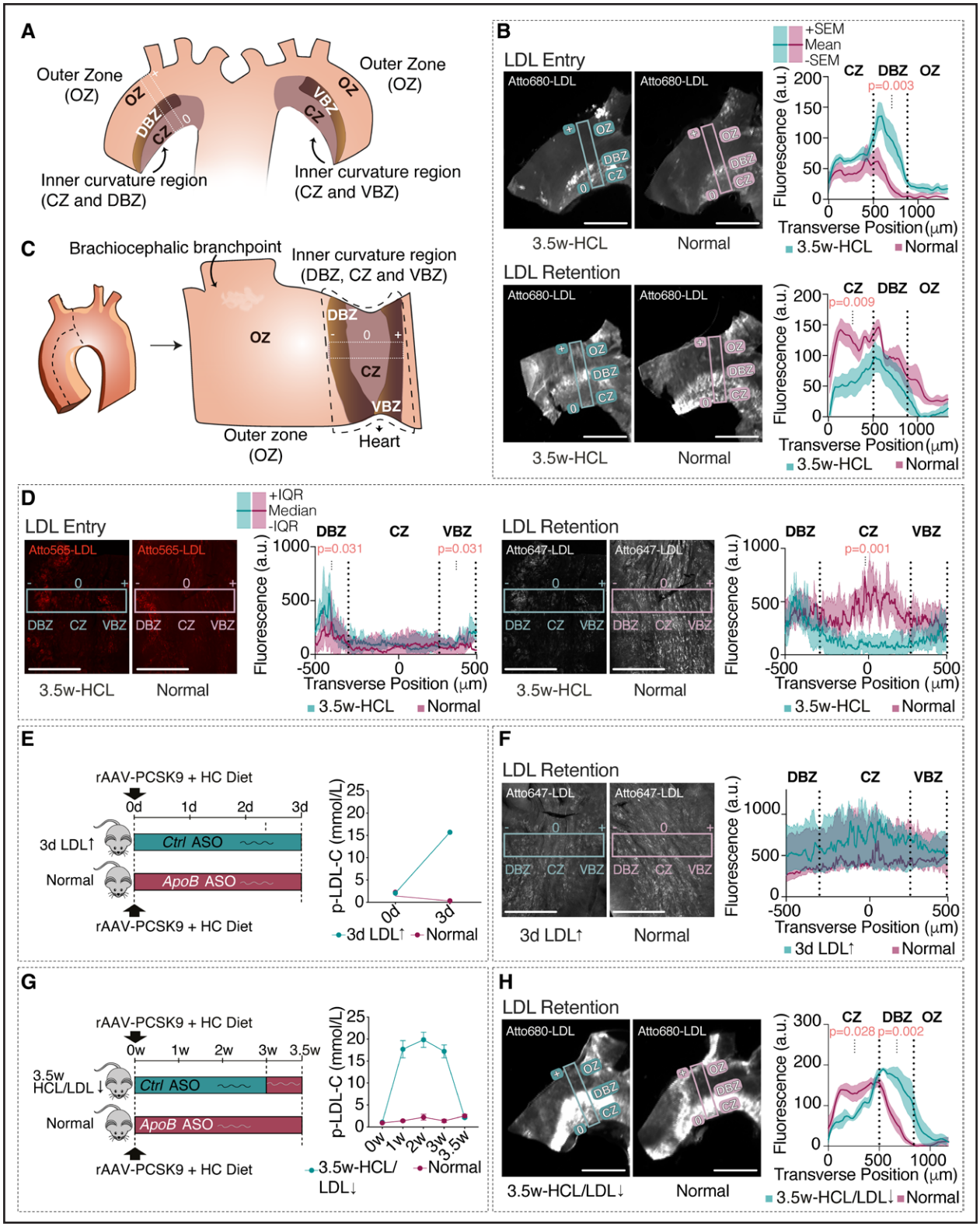

Figure 3. LDL (low-density lipoprotein) entry and retention vary over the inner curvature region.
A, Division of the left (dorsal) section of the opened ascending aortic arch: central zone (CZ), dorsal border zone (DBZ), and outer zone (OZ). **B**, Representative images and quantitative analysis of Atto680-LDL entry and retention across the subdivisions of the inner curvature region. Intensity profiles were measured close to the branch point of the brachiocephalic trunk along the indicated line. The area-under-the-curve within zones was calculated for each mouse and compared between groups. Same mice as in Figure 2A through 2F (n=7–9 per group). **C**, Opening of the aorta for whole-mount microscopy and subdivision of the inner curvature region. **D**, Representative images and quantitative analysis of Atto647-LDL retention (gray) and Atto565-LDL entry (red) after 3.5 weeks of hypercholesterolemia (3.5w-HCL, n=9) (*Continued*)

To confirm these ad hoc findings, we established new groups of mice subjected to 3.5 weeks of normo- or hypercholesterolemia (*study 4*, experimental design as in Figure 2A). Mice were injected with Atto647-LDL and Atto565-LDL at 18 hours and 1 hour before euthanasia and perfusion-fixation, for simultaneous measurements of entry and retention, and the arches were opened in a way that allowed whole-mount microscopy of the full inner curvature region (Figure 3C). Intensity profiles across the inner curvature region confirmed that retained Atto647-LDL was significantly reduced in the central zone of the aortas of hypercholesterolemic versus normocholesterolemic mice, despite similar rates of Atto565-LDL entry (Figure 3D). In contrast, Atto647-LDL retention was maintained in both dorsal and ventral border zones, which also showed higher rates of Atto565-LDL entry.

The combined observations indicate that the dynamics of LDL entry and retention differ greatly across the inner curvature region, which has previously been considered a homogenous atherosclerosis-prone region. In hypercholesterolemia, the increased entry and maintained retention of exogenous labeled LDL in border zones, and its maintained entry and lowered retention in the central zone, indicate that retention is the rate-limiting process for LDL accumulation at all sites. However, the capacity for continued LDL retention differs substantially between them. The central zone has limited capacity, while retention of exogenous labeled LDL in the border zones continues at a high pace during hypercholesterolemia and early atherosclerosis.

The Capacity for LDL Retention Declines in the Central Zone

We next sought to determine if the central zone of early atherosclerotic aortas develops an absolute decline in LDL retention capacity compared with normal aortas. To make that conclusion, we had to exclude the possibility that the observed reduction in the retention signal was explained by differences in circulating LDL levels. If LDLs compete for retention in the central zone, high plasma LDL levels in hypercholesterolemic mice could by itself reduce retention of injected labeled LDLs. We performed 2 experiments to assess the importance of competition from circulating endogenous LDL.

First, we measured labeled LDL retention rates shortly after the induction of hypercholesterolemia. Groups of mice were injected with rAAV-PCSK9, started on HC diet, and given a single injection of *ApoB* or *Ctrl* ASO (*study 5*). After 3 days with high or normal LDL plasma levels, Atto647-LDL was injected, and retention was analyzed by whole-mount microscopy after 18 hours (Figure 3E). The LDL retention pattern was similar between the 2 groups throughout the inner curvature (Figure 3F). This shows that the inner curvature region of the normal aorta initially has such a high capacity for LDL retention that there is no competition for retention among the LDLs that enter the wall. Therefore, the reduction in labeled LDL retention that develops in the central zone after 3.5 weeks of hypercholesterolemia cannot solely be explained by competition among circulating LDLs. The experiment also showed that the reduced capacity for LDL retention takes some time to develop.

Second, we tested whether reduced retention of labeled LDL in the central zone of early atherosclerotic aortas remained if circulating LDL levels were normalized shortly before the measurement. For this, we subjected mice to 3.5 weeks of normo- or hypercholesterolemia but normalized LDL levels in hypercholesterolemic mice 3 days before the retention assay with a single high-dose of *ApoB* ASO (*study 6*, Figure 3G). Retention of Atto680-LDL increased in the dorsal border zone when competition from unlabeled plasma LDL was reduced, but the lower Atto680-LDL retention in the central zone was maintained (Figure 3H). This again confirms that the capacity for LDL retention declines in the central zone of the inner curvature region during the early LDL-accumulating phase of atherosclerosis.

Potential Mechanisms Underlying Reduced LDL Retention in the Central Zone

The decline in LDL retention in the central zone could be caused by the downregulation of proteins involved in binding or precipitating LDLs in the arterial intima. It could also result from simple saturation of a limited number of LDL-binding sites in the intima that were increasingly occupied by accumulating LDLs. To explore these hypotheses, we repeated the standard 3.5-week experiment to produce three additional batches of early atherosclerotic and normal aortas following the experimental design shown in Figure 2A.

From the first batch (*study 7*), we sectioned the ascending aortic arch and stained for proteins involved in LDL

Figure 3 Continued. or normocholesterolemia (normal, n=6). Intensities were measured across the inner curvature region along the indicated line and the area-under-the-curve within zones was calculated for each mouse and compared between groups. **E**, Experimental design. Groups of mice were injected with rAAV (recombinant adeno-associated virus)-PCSK9 (proprotein convertase subtilisin/kexin type 9), fed on high cholesterol (HC) diet, and given a single injection of either *Ctrl* ASO (3d LDL↑, n=5) or *ApoB* ASO (normal, n=5). LDL retention was measured after 3 days. **F**, Representative images and quantitative analysis of Atto647-labeled LDL retention (gray) across the inner curvature region. Analyzed as in **D**. **G**, Experimental design. Groups of rAAV-PCSK9-injected mice were fed on HC diet for 3.5 weeks. One group received *ApoB* ASO at 0, 1, 2, and 3 weeks (normal, n=9), while the other received *Ctrl* ASO at 0, 1, and 2 weeks followed by a final dose of *ApoB* ASO at 3 weeks (n=5, 3.5w-HCL/LDL↓). **H**, Representative near-infrared scans and quantitative analysis of Atto680-LDL retention. Analyzed as in **B**. All, The intensity profile graphs consist of a thick line that indicates the group mean (**B** and **H**) or median (**D** and **F**) surrounded by a colored area indicating ±SEM (**B** and **H**) or ±interquartile range (**D** and **F**), respectively. Graphs in **E** and **G** show mean±SEM. Data analyzed by *t* test (**B** and **H**) and Mann-Whitney *U* test (**D** and **F**). No test performed (**E** and **G**). Scale bars, 1 mm (**B** and **H**), 500 µm (**D** and **F**).

entry (caveolin-1) and retention (perlecan, lipoprotein lipase, and sphingomyelinase; Figure 4A).[2] This batch of mice was injected with Atto647-LDL to mark the inner curvature region. Caveolin-1, perlecan, sphingomyelinase, and lipoprotein lipase were all upregulated in the inner curvature region compared with the outer zone in hypercholesterolemic mice, consistent with their involvement in LDL entry and retention. Only perlecan significantly increased in hypercholesterolemic compared with normal aortas, and the increase was evident in the inner curvature region. More detailed analysis of the signal intensity along the inner curvature region showed that the increase in perlecan was confined to the dorsal border zone, while none of the analyzed proteins showed significant regulation in the central zone in early atherosclerosis (Figure S9).

From the second batch (*study 8*), we isolated the inner curvature region and conducted RNA sequencing. No regulation of mRNAs encoding known LDL-retaining

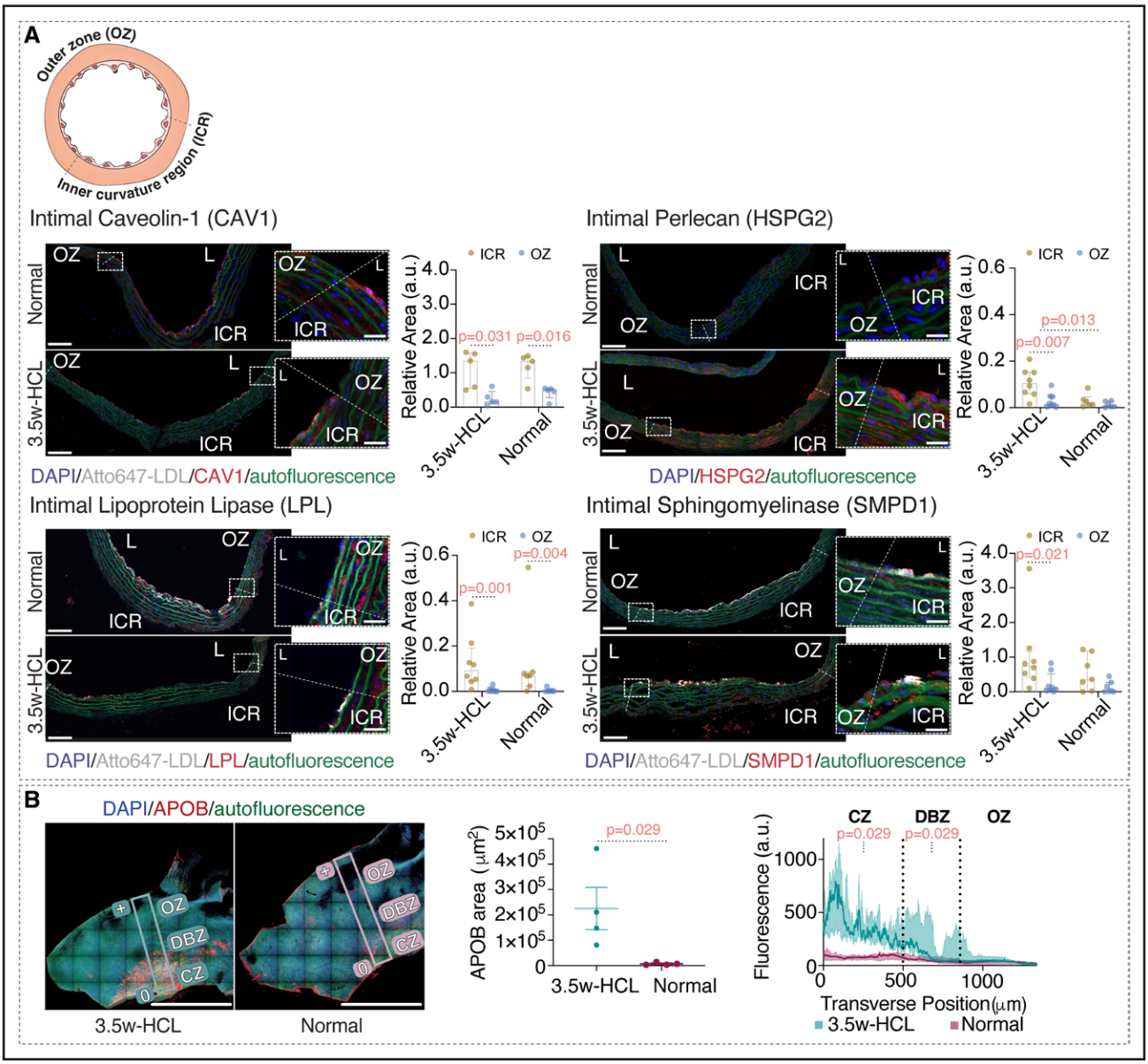

Figure 4. Potential mechanisms behind reduced LDL (low-density lipoprotein) retention in the central zone.
A, Representative images and quantification of immunostainings (red) for CAV1 (caveolin-1), perlecan (HSPG2), LPL (lipoprotein lipase), and SMPD1 (sphingomyelinase) in the inner curvature region (ICR) and neighboring regions of the outer zone (OZ) after 3.5 weeks of hypercholesterolemia (3.5w-HCL) and normocholesterolemia (normal). High-magnification images at the boundary between the ICR and OZ are shown. Atto647-LDL (gray) was injected 1 hour before the endpoint in mice used for CAV1 analysis (n=5 per group) and at 18 hours before in mice used for the other stainings (n=7-8 per group). It is not shown for perlecan staining because of partial deterioration of fluorescence signal by the necessary pretreatment. **B**, Whole-mount microscopy analysis of endogenous LDL accumulation (APOB staining, red) after 3.5 weeks of hypercholesterolemia (3.5w-HCL, n=4) or normocholesterolemia (normal, n=4). No injection of labeled LDL. Comparison of the intensity profile between groups was performed using areas-under-the-curve within each zone. All, Graphs show median±interquartile range. Data analyzed by Mann-Whitney *U* test. Scale bars, 100 μm in overview and 20 μm in higher magnification images (**A**), 1 mm (**B**).

proteins was observed, but we obtained evidence that early atherosclerotic arches from hypercholesterolemic mice were overloaded with cholesterol, for example, downregulation of *Ldlr,* upregulation of *Abca1*, and overrepresentation of lipid metabolism in Ingenuity Pathway Analysis (Figure S10; Table S1). Among the most significant predicted upstream regulators, the ingenuity pathway analysis identified SREBF2, whose inhibition would explain the upregulation of *Abca1* and downregulation of *Ldlr*. *Srebf2* was also downregulated at the mRNA level.

Having not seen regulation on the protein or mRNA level that could explain reduced LDL retention in the central zone, we turned to investigate if there was local LDL accumulation that could saturate binding sites for incoming LDL. To this end, we stained the third batch (*study 9*) of aortic arches for APOB and analyzed them by whole-mount microscopy. Accumulation of endogenous LDL was abundant in the central zone after 3.5 weeks of hypercholesterolemia and even numerically more pronounced than in border zones (Figure 4B).

These findings suggest that the capacity to retain exogenous labeled LDL declines in the central zone in early atherosclerosis owing to 3.5 weeks of saturation of available binding sites by endogenous LDL. This is not the case for border zones, where the combination of high rates of LDL retention and only moderate buildup of LDL suggests higher local turnover of retained LDL.

LDL Retention Capacity Predicts the Temporal Course of Plaque Development

We next asked if the differences in LDL retention capacity in the inner curvature region associate with atherosclerosis susceptibility. First, we looked for signs of early macrophage accumulation in aortic arches that we had previously analyzed for LDL retention after 3.5 weeks of hyper- or normocholesterolemia (*study 4*, Figure 3D). Post-staining for the macrophage marker galectin-3 (LGALS3 aka. Mac2) showed accumulation of macrophages in the border zones after 3.5 weeks of hypercholesterolemia, while in the central zone, macrophage content remained comparable to that in normal aortas (Figure 5A). Initial macrophage accumulation therefore correlated well with high Atto-647-LDL retention in early atherosclerotic aortas (Figure 5B). Both Atto647-LDL retention and macrophage accumulation tended to be stronger in the dorsal than in the ventral border zone at this time point.

To study the topography of subsequent plaque formation, we fed rAAV-PCSK9-injected mice on HC diet for 0, 4, 6, 12, or 24 weeks (*study 10*) and examined arches qualitatively by stereomicroscopy (Figure 5C through 5E). Plaque formation was first evident at 6 weeks, where they appeared in the V-shaped border zones of the inner curvature. At 12 weeks of atherogenesis, plaques started to incorporate the central zone of the inner curvature until completely covering it at 24 weeks (Figure 5E and 5F and additional examples in Figure S11). The outer zone did not develop atherosclerosis over 24 weeks of hypercholesterolemia.

Capacity for LDL Retention Is Substantially Increased in Plaques

Finally, we asked if the barrier to continued LDL retention in the central zone was lost upon conversion to atherosclerotic plaque. We induced atherosclerotic plaques in two groups of rAAV-PCSK9-injected mice fed on HC diet for 12 weeks. The last week before the endpoint, we created a large difference in plasma LDL by injecting one group with *ApoB* ASO and the other with *Ctrl* ASO (*study 11*, Figure 6A and 6B). Atto647-LDL was injected 18 hours before the end point, and retention in the plaque and residual nonplaque intima of the inner curvature region was analyzed in aortic arch sections by confocal microscopy (Figure 6C). The rationale was that increased retention of Atto647-LDL after removing competition from endogenous LDLs would indicate a saturable, low-capacity process.

Like others in a similar model,[15] we found no change in plaque size or macrophage content (Figure 6D and 6E). Nonplaque regions of the inner curvature region had increased Atto647-LDL retention when competition from circulating endogenous LDLs was removed. This indicated, consistent with our findings in early atherosclerosis, a limited capacity for LDL retention in these areas. In contrast, no difference in Atto647-LDL retention was present in atherosclerotic plaques indicating a high capacity for retention that is not saturated at high plasma LDL levels in the PCSK9-induced atherosclerosis model (>20 mmol/L; Figure 6F and 6G).

Combining our findings at different stages of atherogenesis in the murine aortic arch, we have thus found that the atherosclerosis-prone inner curvature region initially has a high capacity for LDL retention, but that retention is saturated to a varying degree in early hypercholesterolemia, before returning to high capacity in atherosclerotic plaques.

DISCUSSION

The focal pattern of atherogenesis is a striking feature. Lesions develop near branch sites and on the inside of arterial curvatures, while other regions of the arterial tree are long protected. The accumulation of LDL at these atherosclerosis-prone sites causes atherosclerosis onset, but why LDL accumulates there and not elsewhere remains uncertain.[2]

Various studies have implicated either increased LDL entry or increased intimal LDL retention as the distinguishing feature of susceptible arterial regions. Using radiolabeled LDL in rabbits, one study found that atherosclerosis-susceptible aortic regions were characterized

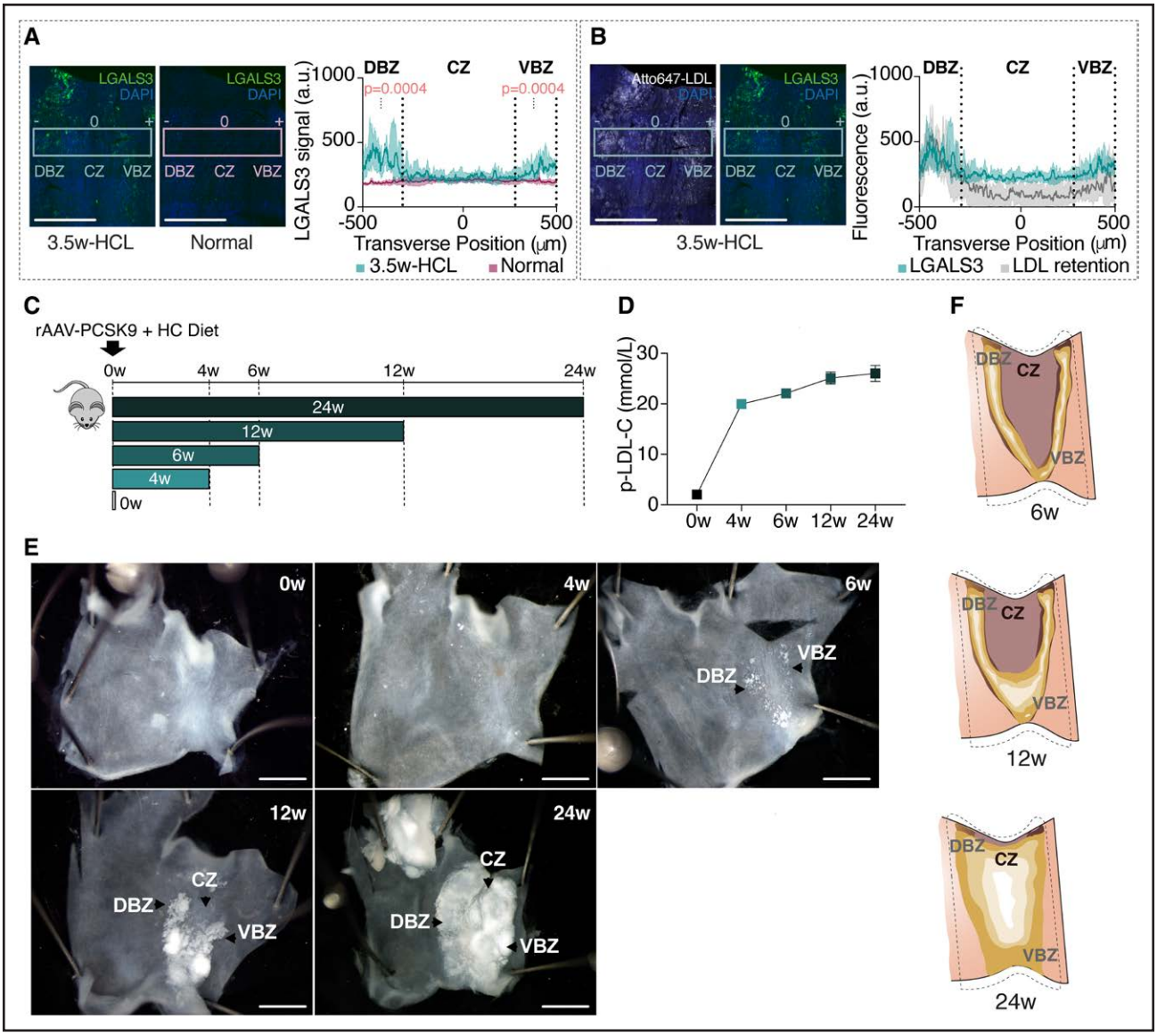

Figure 5. Topography of macrophage accumulation and atherogenesis.
A, Analysis of macrophage distribution (LGALS3 staining, green) after 3.5 weeks of high (3.5w-HCL, n=9) or normal (normal, n=6) plasma LDL (low-density lipoprotein) levels. Intensity profiles were measured along the indicated line across the inner curvature region. Area-under-the-curve within zones for individual mice were compared between groups. **B**, Colocalization of LGALS3 and Atto647-LDL retention signal (gray) in the 3.5w-HCL group (n=9). **C**, Experimental design. rAAV (recombinant adeno-associated virus)-PCSK9 (proprotein convertase subtilisin/kexin type 9)-injected mice were fed on high cholesterol (HC) diet for 0 (n=4), 4 (n=5), 6 (n=6), 12 (n=6), or 24 weeks (n=6). **D**, Plasma LDL cholesterol concentration. **E**, Representative stereomicroscope images of the inner aortic arch. Border and central zones with atherosclerosis are indicated with black arrowheads. **F**, Schematic representation of the topography of plaque development after 6, 12, and 24 weeks of hypercholesterolemia. All, Graphs show median±interquartile range (**A** and **B**) or mean±SEM (**D**). Data analyzed by Mann-Whitney *U* test (**A** and **B**). No test performed (**D**). Scale bars, 500 μm (**A** and **B**), 1 mm (**E**).

by higher LDL retention, but not higher entry.[5] Another, conversely, that atherosclerosis-prone regions are marked by higher LDL entry.[6]

Arguments for the importance of one or the other process can also be found in functional studies. Knockout of *Caveolin-1*, which lowers LDL transcytosis through endothelial cells, inhibits atherosclerosis.[16] However, early atherogenesis is also retarded by inhibiting LDL retention through the disruption of LDL-proteoglycan binding or intimal LDL aggregation[2,4]; moreover, in cases where manipulations had discordant effects on LDL entry and retention, the effect on atherogenesis appeared to be dominated by the effect on LDL retention.[2,17] Furthermore, experimental manipulation of blood flow that increases atherosclerosis susceptibility in mouse carotids increased LDL retention but not LDL entry.[10] These intervention studies show that both LDL entry and LDL retention are regulatable steps in LDL accumulation, but they do not speak to which is the rate-limiting mechanism during the natural history of atherosclerosis.

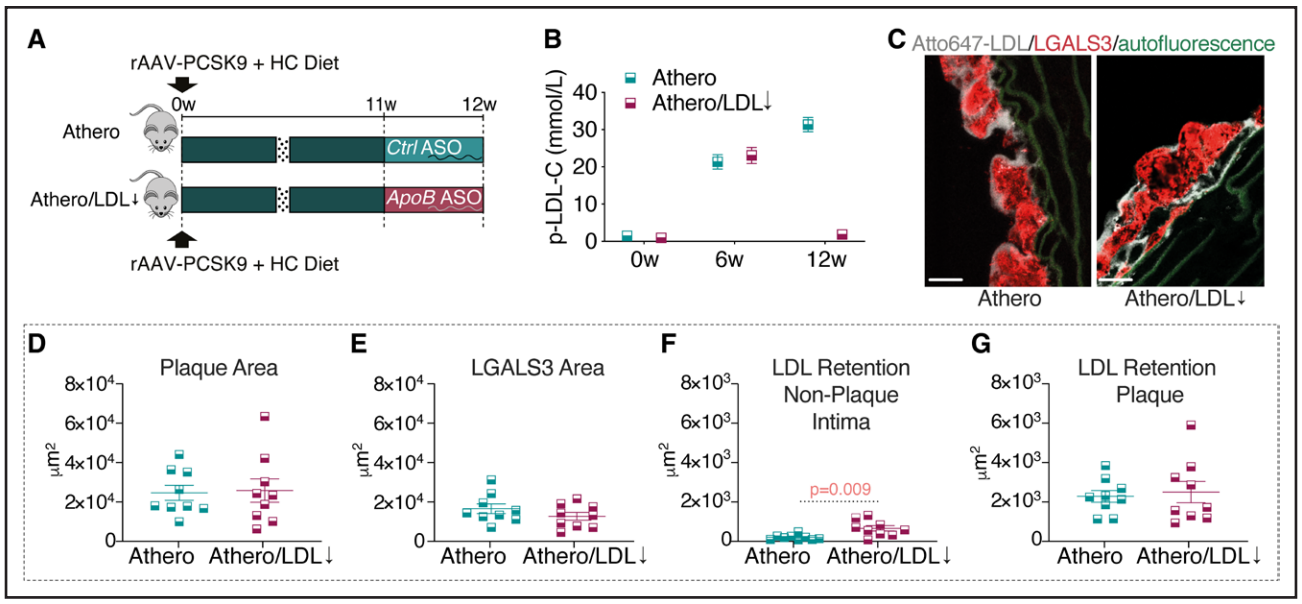

Figure 6. High capacity for LDL (low-density lipoprotein) retention in atherosclerotic plaques.
A, Experimental design. Mice were injected with rAAV (recombinant adeno-associated virus)-PCSK9 (proprotein convertase subtilisin/kexin type 9) and fed on high cholesterol (HC) diet for 12 weeks. A week before the endpoint, one group received *ApoB* ASO (Athero/LDL↓, n=9) and the other *Ctrl* ASO (Athero, n=9). **B**, Plasma LDL cholesterol concentrations. **C**, Representative images of aortic arch sections showing Atto647-LDL retention (gray), LGALS3+ macrophages (red), and autofluorescence (green). **D** and **E**, Quantification of plaque and LGALS3+ macrophage area. **F** and **G**, Quantification of Atto647-LDL retention area in nonplaque intima and atherosclerotic plaques in the inner curvature region. All, Graphs show mean±SEM. Data analyzed by *t* test (**D**–**F**) or Welch *t* test (**G**). Scale bars, 20 μm.

The present study delivers a systematic analysis of LDL dynamics in the mouse aortic arch during early atherogenesis. We report entry and retention rates across susceptible and resistant regions and contrast them between normal arteries and arteries developing atherosclerosis. The approach goes beyond previous analyses by providing higher resolution and by using methods that allowed us to compare mice with high and normal plasma LDL without creating differences in the clearance of the labeled LDL probe. We report the following main findings:

First, differences in LDL entry and retention rates in the normal (non-atherosclerotic) mouse aortic arch divide it into three regions with differing atherosclerosis susceptibility. The resistant zone in the outer part of the arch takes up and retains little LDL and develops no atherosclerosis over 24 weeks of hypercholesterolemia. The intermediate-susceptibility zone in the central part of the inner curvature region retains LDL but does not have a high average rate of LDL entry; this zone is initially unaffected by atherosclerosis but develops it over 6 to 24 weeks. Finally, the highly susceptible dorsal and ventral border zones lie between the resistant and intermediate-susceptibility regions; these regions have high rates of both entry and retention and are the location where lesions are initiated. These observations offer a unifying explanation for previous studies that have variably associated subsequent atherosclerosis development with the pattern of LDL entry or retention. We find that both LDL entry and retention in normal aortas are associated with atherosclerosis susceptibility but with different time horizons. High LDL entry characterizes the border zones where atherosclerosis develops first, whereas the pattern of retention predicts the surface area that will be covered with lesions in the long term. To the best of our knowledge, the regional differences observed in the inner curvature region have not been reported before.

Why these regional differences exist within the inner curvature requires further investigation. Flow forces are important in controlling inflammation and LDL retention in arteries,[10] and it is possible that differences in flow velocities and direction, which can vary over short distances, is the underlying cause. To our knowledge, flow has not yet been mapped at sufficient resolution in the murine aortic arch to test this hypothesis.

Second, we find that LDL retention is the rate-limiting process for LDL accumulation, both at the global level and within the subdivisions of the inner curvature region. This conclusion is based on several experiments that compared early atherosclerotic and normal aortas and found increased entry combined with reduced or unchanged retention (at the global level and in border zones, respectively) or maintained entry combined with reduced retention (in the central zone). Both indicate that LDLs enter in excess and that it is the efficiency of retention that determines how many accumulate. These observations are consistent with many previous observations, including direct dynamic studies of outflow from perfused atherosclerotic rabbit aortas.[2,3]

Third, we find that the capacity to continue LDL retention varies substantially among the subdivisions of the

inner curvature region. The central zone undergoes a phase in which LDL accumulation is slowed down. This is due to intrinsic changes—not explained solely by increased competition from circulating LDLs—and it occurs without conspicuous regulation of known LDL-retaining proteins. Therefore, the most likely mechanism is the saturation of available binding sites in the intimal matrix, which is consistent with abundant accumulation of endogenous LDLs in this region.

In contrast, the border zones increased their capacity to retain LDL over the first 3.5 weeks of hypercholesterolemia, which could be seen by the higher retention of labeled LDL when competition from circulating LDLs was briefly normalized. This trait was associated with the presence of macrophages, increases in LDL entry, and increased perlecan expression. Previous studies have shown that the rate of LDL degradation is increased in active atherosclerotic plaques.[18] One may speculate that the recruitment of macrophages to the border zones facilitates continued high LDL retention by removing extracellular LDL and clearing binding sites for new incoming LDL. This is a potential mechanism by which inflammation and LDL retention converge to create futile retention and degradation cycles leaving behind nondegradable and proinflammatory cholesterol. That said, although LDL retention long precedes macrophage recruitment, we cannot determine in the present study whether increased retention occurred because of macrophage recruitment, or vice versa.

Finally, we find that the barriers to LDL retention in the inner curvature region disappear upon conversion to atherosclerotic plaques. A much higher capacity for LDL retention in plaque compared with nonplaque areas has been previously demonstrated in atherosclerotic rabbit and murine aortas.[3,18,19] Still, it is notable that even at the excessive plasma LDL levels of rAAV-PCSK9-injected and HC-fed mice, we saw no signs of competition for LDL retention. In addition to macrophage-mediated clearing of binding sites, as discussed above, it is known that LDL retention mechanisms shift once lesions are initiated; direct binding of APOB to arterial proteoglycans loses importance, and other types of retention take over, for example, via binding to lipoprotein lipase[19] or through enzyme-catalyzed aggregation.[20] These mechanisms may have a higher capacity to retain LDL in the intima than APOB-proteoglycan binding. Also, potentially important is the increased distribution volume for incoming LDL in plaques compared with non-diseased arteries and decreased pH in the plaque interior, which may facilitate APOB-proteoglycan binding and LDL aggregation. Understanding the molecular basis for the substantial variations in LDL entry and retention over short aortic distances and how they evolve during atherogenesis are important areas for future studies.

Limitations

Our experiments have limitations that should be considered. First, the human LDLs that we used as probes may differ from murine LDLs in binding affinity to LDL-handling receptors and enzymes in the arterial wall, as they do for binding to the murine LDL receptor.[18,21–23] Having said that, LDLs with human APOB are fully capable of being retained and causing atherosclerosis in mice.[24] Second, the experiments where LDL levels were rapidly altered to introduce or remove competition could be biased by concomitant regulation of retention mechanisms in the arterial wall. We did not find evidence for such regulation in the central zone during the early LDL-accumulating phase by immunostaining or RNA sequencing, but the situation is more complex for established atherosclerotic plaques. Bartels et al[15] examined total aortic LDL entry, retention, and degradation in atherosclerotic *Ldlr* knockout mice subjected to 1 week of LDL lowering. They did not find changes in the retention of intact radioactive LDL after 24 hours, but both LDL entry and degradation were decreased. Similar changes in our advanced atherosclerosis experiment could in principle have masked an increase in retention caused by reduced competition from endogenous LDL, although it remains a simpler explanation that no such competition exists. Third, humans have considerably thicker intima than mice at atherosclerosis-prone sites, which may entail much higher capacity for continued LDL retention. This should be considered before attempting to translate our findings to human atherosclerosis.

Conclusions

Retention is the limiting mechanism for LDL accumulation in the murine aortic arch, but the capacity for LDL retention varies substantially over surprisingly short distances within the inner curvature, usually considered a uniformly atherosclerosis-prone region. High capacity for continued LDL retention marks areas with imminent atherosclerosis. Low-capacity regions are temporarily protected but develop atherosclerosis later.

ARTICLE INFORMATION

Received October 18, 2022; accepted January 31, 2023.

Affiliations

Experimental Pathology of Atherosclerosis, Centro Nacional de Investigaciones Cardiovasculares Carlos III, Madrid, Spain (E.A.L., R.M.-A., I.R.-A., L.G.-C., J.F.B.). Heart Diseases and Steno Diabetes Center Aarhus, Department of Clinical Medicine, Aarhus University, Denmark (E.A.L., L.G.-C., J.F.B.). Unit of Microscopy and Dynamic Imaging, Centro Nacional de Investigaciones Cardiovasculares Carlos III, Madrid, Spain (V.L.-C.).

Acknowledgments

We thank the CNIC (Centro Nacional de Investigaciones Cardiovasculares Carlos III) Viral Vector Unit, Microscopy Unit, Histology Unit, Genomics Unit, Bioinformatics Unit, and Animal Facility for their excellent technical assistance, and Simon Bartlett, CNIC, for English editing.

Sources of Funding

This study was supported by grants from the Ministerio de Economía, Industria y Competitividad (MEIC) with cofunding from the European Regional Development Fund (SAF2016-75580-R and PID2019-108568RB-I00), the Novo Nordisk Foundation (NNF17OC0030688) and the La Caixa Health Research Programme (HR20-00075, AtheroConvergence). V. Labrador-Cantarero is supported by FEDER "Una manera de hacer Europa" for the project In Vivo Advanced Nanoscopy at the ICTS–ReDib–TRIMA–CNIC. CNIC is supported by the Instituto de Salud Carlos III (ISCIII), the Ministerio de Ciencia e Innovación, and the Pro CNIC Foundation and is a Severo Ochoa Center of Excellence (SEV-2015-0505).

Disclosures

None.

Supplemental Material

Expanded Methods
Figures S1–S11
Table S1
Major Resources Tables
References[25–29]

REFERENCES

1. Borén J, Chapman MJ, Krauss RM, Packard CJ, Bentzon JF, Binder CJ, Daemen MJ, Demer LL, Hegele RA, Nicholls SJ, et al. Low-density lipoproteins cause atherosclerotic cardiovascular disease: pathophysiological, genetic, and therapeutic insights: a consensus statement from the European atherosclerosis society consensus panel. *Eur Heart J*. 2020;41:2313–2330. doi: 10.1093/eurheartj/ehz962
2. Borén J, Williams KJ. The central role of arterial retention of cholesterol-rich apolipoprotein-B-containing lipoproteins in the pathogenesis of atherosclerosis: a triumph of simplicity. *Curr Opin Lipidol*. 2016;27:473–483. doi: 10.1097/MOL.0000000000000330
3. Björnheden T, Bondjers G, Wiklund O. Direct assessment of lipoprotein outflow from in vivo-labeled arterial tissue as determined in an in vitro perfusion system. *Arterioscler Thromb Vasc Biol*. 1998;18:1927–1933. doi: 10.1161/01.atv.18.12.1927
4. Skålén K, Gustafsson M, Rydberg EK, Hultén LM, Wiklund O, Innerarity TL, Borén J. Subendothelial retention of atherogenic lipoproteins in early atherosclerosis. *Nature*. 2002;417:750–754. doi: 10.1038/nature00804
5. Schwenke DC, Carew TE. Initiation of atherosclerotic lesions in cholesterol-fed rabbits. II. Selective retention of LDL vs. selective increases in LDL permeability in susceptible sites of arteries. *Arteriosclerosis*. 1989;9:908–918. 10.1161/01.atv.9.6.908
6. Nielsen LB. Transfer of low density lipoprotein into the arterial wall and risk of atherosclerosis. *Atherosclerosis*. 1996;123:1–15. doi: 10.1016/0021-9150(96)05802-9
7. Robinet P, Milewicz DM, Cassis LA, Leeper NJ, Lu HS, Smith JD. Consideration of sex differences in design and reporting of experimental arterial pathology studies—statement from ATVB council. *Arterioscler Thromb Vasc Biol*. 2018;38:292–303. doi: 10.1161/ATVBAHA.117.309524
8. Bjørklund MM, Hollensen AK, Hagensen MK, Dagnæs-Hansen F, Christoffersen C, Mikkelsen JG, Bentzon JF. Induction of atherosclerosis in mice and hamsters without germline genetic engineering. *Circ Res*. 2014;114:1684–1689. doi: 10.1161/circresaha.114.302937
9. Straarup EM, Fisker N, Hedtjarn M, Lindholm MW, Rosenbohm C, Aarup V, Hansen HF, Orum H, Hansen JBR, Koch T. Short locked nucleic acid antisense oligonucleotides potently reduce apolipoprotein B mRNA and serum cholesterol in mice and non-human primates. *Nucleic Acids Res*. 2010;38:7100–7111. doi: 10.1093/nar/gkq457
10. Steffensen LB, Mortensen MB, Kjolby M, Hagensen MK, Oxvig C, Bentzon JF. Disturbed laminar blood flow vastly augments lipoprotein retention in the artery wall: a key mechanism distinguishing susceptible from resistant sites. *Arterioscler Thromb Vasc Biol*. 2015;35:1928–1935. doi: 10.1161/ATVBAHA.115.305874
11. Schindelin J, Arganda-Carreras I, Frise E, Kaynig V, Longair M, Pietzsch T, Preibisch S, Rueden C, Saalfeld S, Schmid B, et al. Fiji: an open-source platform for biological-image analysis. *Nat Methods*. 2012;9:676–682. doi: 10.1038/nmeth.2019
12. Ruifrok AC, Johnston DA. Quantification of histochemical staining by color deconvolution. *Anal Quant Cytol Histol*. 2001;23:291–299.
13. Nievelstein PF, Fogelman AM, Mottino G, Frank JS. Lipid accumulation in rabbit aortic intima 2 hours after bolus infusion of low density lipoprotein. A deep-etch and immunolocalization study of ultrarapidly frozen tissue. *Arterioscler Thromb J Vasc Biol* 1991;11:1795–1805. doi: 10.1161/01.atv.11.6.1795
14. Bragdon J. Transfusion transfer of experimental atherosclerosis. *Circulation*. 1951;4:466.
15. Bartels ED, Christoffersen C, Lindholm MW, Nielsen LB. Altered metabolism of LDL in the arterial wall precedes atherosclerosis regression. *Circ Res*. 2015;117:933–942. doi: 10.1161/CIRCRESAHA.115.307182
16. Ramírez CM, Zhang X, Bandyopadhyay C, Rotllan N, Sugiyama MG, Aryal B, Liu X, He S, Kraehling JR, Ulrich V, et al. Caveolin-1 regulates atherogenesis by attenuating low-density lipoprotein transcytosis and vascular inflammation independently of endothelial nitric oxide synthase activation. *Circulation*. 2019;140:225–239. doi: 10.1161/CIRCULATIONAHA.118.038571
17. Tran-Lundmark K, Tran P-K, Paulsson-Berne G, Friden V, Soininen R, Tryggvason K, Wight TN, Kinsella MG, Boren J, Hedin U. Heparan sulfate in perlecan promotes mouse atherosclerosis: roles in lipid permeability, lipid retention, and smooth muscle cell proliferation. *Circ Res*. 2008;103:43–52. doi: 10.1161/CIRCRESAHA.108.172833
18. Björnheden T, Babyi A, Bondjers G, Wiklund O. Accumulation of lipoprotein fractions and subfractions in the arterial wall, determined in an in vitro perfusion system. *Atherosclerosis*. 1996;123:43–56. doi: 10.1016/0021-9150(95)05770-6
19. Gustafsson M, Levin M, Skålén K, Perman J, Fridén V, Jirholt P, Olofsson S-O, Fazio S, Linton MF, Semenkovich CF, et al. Retention of low-density lipoprotein in atherosclerotic lesions of the mouse: evidence for a role of lipoprotein lipase. *Circ Res*. 2007;101:777–783. doi: 10.1161/CIRCRESAHA.107.149666
20. Devlin CM, Leventhal AR, Kuriakose G, Schuchman EH, Williams KJ, Tabas I. Acid sphingomyelinase promotes lipoprotein retention within early atheromata and accelerates lesion progression. *Arterioscler Thromb Vasc Biol*. 2008;28:1723–1730. doi: 10.1161/ATVBAHA.108.173344
21. Corsini A, Mazzotti M, Villa A, Maggi FM, Bernini F, Romano L, Romano C, Fumagalli R, Catapano AL. Ability of the LDL receptor from several animal species to recognize the human apo B binding domain: studies with LDL from familial defective apo B-100. *Atherosclerosis*. 1992;93:95–103. doi: 10.1016/0021-9150(92)90203-s
22. Sneck M, Nguyen SD, Pihlajamaa T, Yohannes G, Riekkola M-L, Milne R, Kovanen PT, Oörni K. Conformational changes of apoB-100 in SMase-modified LDL mediate formation of large aggregates at acidic pH. *J Lipid Res*. 2012;53:1832–1839. doi: 10.1194/jlr.M023218
23. Glise L, Rutberg M, Håversen L, Levin MC, Levin M, Jeppsson A, Borén J, Fogelstrand P. pH-dependent protonation of histidine residues is critical for electrostatic binding of low-density lipoproteins to human coronary arteries. *Arterioscler Thromb Vasc Biol*. 2022;42:1037–1047. doi: 10.1161/ATVBAHA.122.317868
24. Purcell-Huynh DA, Farese RV, Johnson DF, Flynn LM, Pierotti V, Newland DL, Linton MF, Sanan DA, Young SG. Transgenic mice expressing high levels of human apolipoprotein B develop severe atherosclerotic lesions in response to a high-fat diet. *J Clin Invest*. 1995;95:2246–2257. doi: 10.1172/JCI117915
25. Babraham bioinformatics - FastQC a quality control tool for high throughput sequence data [Internet]. [cited 2021 Apr 1];Available from: https://www.bioinformatics.babraham.ac.uk/projects/fastqc/
26. Martin M. Cutadapt removes adapter sequences from high-throughput sequencing reads. *EMBnet J*. 2011;17:10. doi: 10.14806/ej.17.1.200
27. Li B, Dewey CN. RSEM: accurate transcript quantification from RNA-Seq data with or without a reference genome. *BMC Bioinf*. 2011;12:323. doi: 10.1186/1471-2105-12-323
28. Ritchie ME, Phipson B, Wu D, Hu Y, Law CW, Shi W, Smyth GK. limma powers differential expression analyses for RNA-sequencing and microarray studies. *Nucleic Acids Res*. 2015;43:e47. doi: 10.1093/nar/gkv007
29. Krämer A, Green J, Pollard J, Tugendreich S. Causal analysis approaches in ingenuity pathway analysis. *Bioinforma Oxf Engl*. 2014;30:523–530. doi: 10.1093/bioinformatics/btt703